PERGAMON

International Journal of Solids and Structures 37 (2000) 1483–1499

INTERNATIONAL JOURNAL OF SOLIDS and STRUCTURES

www.elsevier.com/locate/ijsolstr

Free vibration of thick, layered rectangular plates with point supports by finite layer method

D. Zhou[a], Y.K. Cheung[b,*], J. Kong[c]

[a]*School of Mechanical Engineering, Nanjing University of Science and Technology, Nanjing 210014, P.R. China*
[b]*Department of Civil and Structural Engineering, The University of Hong Kong, Pokfulam Road, Hong Kong*
[c]*Maunsell Consultants Asia Ltd, Hong Kong*

Received 6 June 1998; in revised form 29 October 1998

Abstract

In this paper, the free vibration of thick, isotropic and laminated composite rectangular plates with point supports is analyzed by the finite layer method. A new set of two-dimensional basic functions, which satisfies the kinematic boundary conditions at the edges of the plate and the zero-displacement conditions at point supports, is developed to describe the variation of three-dimensional displacements in the plane of a thin finite layer. One-dimensional linear or quadratic shape functions are adopted to describe the variation of the displacements through the thickness layer. The governing eigenvalue equation of the plate is derived via the conventional displacement method. Numerical results for the three-dimensional vibration of rectangular plates with point supports are presented herein for the first time. The eigenfrequencies of simply-supported rectangular plates with a central point-support are studied in detail by considering the variations of aspect ratio, side-to-thickness ratio, properties of materials, number of laminates and stacking sequences. Comparison with known thin-plate and Mindlin-plate solutions is carried out to verify the applicability and accuracy of the proposed method. © 1999 Elsevier Science Ltd. All rights reserved.

1. Introduction

The rectangular plate is one of the most commonly used structural elements in civil, aeronautical and marine engineering. The vibration frequencies are important parameters for the dynamic analysis of structures.

A close scrutiny among the references on dynamic analysis of structural elements reveals that to date, most investigations are about thin plates (Leissa, 1969), while study on vibration of thick plates has received little attention because of the difficulty in expressing the three-dimensional displacement field. The difficulty of three-dimensional analysis renders the rapid development of refined plate theories

* Corresponding author. Fax: +852-2559-5337.

PII: S0020-7683(98)00316-3

(Mindlin, 1951; Reddy, 1984; Hanna and Leissa, 1994). Applying these theories, one can reduce the dimension of problems from three to two by taking certain averages of some parametric quantities, such as membrane forces, bending moments and shear forces, over the smaller dimension (thickness). The Mindlin plate theory (Mindlin, 1951) is formulated by introducing the concept of a shear correction factor to account for the influence of shear deformation on the dynamic properties of the plate. Numerical studies using the Mindlin plates theory (Dave, 1978; Liew et al., 1993) can be found in the literature. However, it should be noted that although the analytical accuracy can be improved by using higher-order theories, the local variation of through-thickness displacements of the plate cannot be exactly represented and thus results in errors which increase with the thickness of the plate. For very thick plates, a three-dimensional elasticity theory is necessary to obtain accurate results. Because of the complexity of the problem, closed-form exact solutions exist only for simply-supported thick rectangular plates (Srinivas et al., 1970). In most cases, approximate analytical and/or numerical methods have to be adopted. It is well-known that the finite element method is an applicable tool to such a problem. However, it requires discretisation in every dimension of the problem and therefore, will require more unknowns for approximation than some other methods. This certainly results in the increase in cost and the requirement of a super-computer. Cheung and Chakrabarti (1972) used the finite layer method and Fan and Sheng (1992) used the analytical method to investigate the free vibration of thick, layered rectangular plates. Leissa and Zhang (1983) and Liew et al. (1993, 1994) used polynomials as trial functions to study the three-dimensional free vibration of isotropic thick rectangular plates by the Rayleigh–Ritz method.

In some practical applications, such as floor slabs, bridge decks and solar panels, interior and edge point-supports are often placed at some locations of the plate to limit the displacements and to achieve a better distribution of stresses and/or to satisfy special architectural and functional requirements. The effects of point supports on the dynamic characteristics of plates have been an interesting subject for many researchers. For thin rectangular plates with point supports, some pioneering studies have been carried out by Fan and Cheung (1984) using the finite strip method, Mizusawa and Kajita (1987) using the spline element method, Kim and Dickinson (1987) using polynomials as trial functions in the Rayleigh–Ritz method and Gorman and Singal (1991) using the analytical superposition method. Recently, Liew et al. (1994) used a set of pb-2 shape functions to study the free vibration of Mindlin plates with point supports. However, no information is currently available for free vibration of three-dimensional thick plates with point supports. The finite layer method (Cheung and Tham, 1997) is used in this paper to investigate the free vibration of thick, layered rectangular plates with point supports. A new set of basic functions is constructed in two parts with the first part being a set of static beam functions under sinusoidal loads, while the second is for beams under point loads. These functions are developed to describe variation of the three-dimensional displacements in the plane of a thin finite layer, while a one-dimensional linear or quadratic shape function is adopted to describe the variation of the displacements through the thickness of the layer. This set of basic functions satisfies the geometric boundary conditions at the edges of the plate and the zero-displacement conditions at the point supports. A simply-supported rectangular plate with a central point-support is taken as an example of numerical application. The influence of aspect ratio, side-to-thickness ratio and various structural parameters on the eigenfrequencies of plates is examined in detail. Some numerical data are tabulated and compared with other thin-plate and Mindlin-plate results and the accuracy has been confirmed by convergence studies.

2. Two sets of static beam functions

In order to study the free vibration of thick rectangular plates with point supports, two sets of one-dimensional static beam functions have to be developed. They will together form a set of two-dimensional basic functions representing the variation of displacements in the plane of a thin finite layer.

2.1. The static beam functions under a series of sinusoidal loads

Consider a beam subject to a series of static sinusoidal loads distributed along the length, the complete solution (Zhou, 1996) may be written as

$$z(\xi) = \sum_{i=1}^{\infty} Q_i \phi_i(\xi) \tag{1a}$$

$$\phi_i(\xi) = B_{0i} + B_{1i}\xi + B_{2i}\xi^2 + B_{3i}\xi^3 + \sin i\pi\xi \tag{1b}$$

where $z(\xi)$ is the deflection of the beam, Q_i denotes the amplitude of the ith sinusoidal load component, ξ $(0 \leqslant \xi \leqslant 1)$ is the non-dimensional coordinate along the beam and B_{ji} $(j = 0, 1, 2, 3)$ are the unknown constants which can be determined by the boundary conditions of the beam (for a beam without rigid body motions) as shown in Table 1.

For a beam with rigid body motions, the coefficients B_{ji} $(j = 0, 1, 2, 3)$ cannot be determined directly by the boundary conditions. In this case, the rigid body modes should be added to the static beam functions. For example, the static beam functions for a F-S beam should be selected as

$$\phi_1(\xi) = 1 - \xi,$$

$$\phi_{i+1}(\xi) = B_{0i} + B_{1i}\xi + B_{2i}\xi^2 + B_{3i}\xi^3 + \sin i\pi\xi, \quad i \geqslant 1 \tag{1c}$$

where B_{ji} $(j = 0, 1, 2, 3)$ are those for the F-C beam. For an S-F beam, the static beam functions should be selected as

$$\phi_1(\xi) = \xi,$$

$$\phi_{i+1}(\xi) = B_{0i} + B_{1i}\xi + B_{2i}\xi^2 + B_{3i}\xi^3 + \sin i\pi\xi, \quad i \geqslant 1 \tag{1d}$$

Table 1
The coefficients of static beam functions under sinusoidal loads

Boundary condition	B_{0i}	B_{1i}	B_{2i}	B_{3i}
S-S	0	0	0	0
C-C	0	$-i\pi$	$i\pi((-1)^i + 2)$	$i\pi((-1)^i + 1)$
C-F	0	$-i\pi$	$-(i\pi)^3(-1)^i/2$	$(i\pi)^3(-1)^i/6$
C-S	0	$-i\pi$	$3i\pi/2$	$-i\pi/2$
F-C	$(-1)^i(i\pi)[(i\pi)^2/3 + 1]$	$-(-1)^i(i\pi)[(i\pi)^2/2 + 1]$	0	$(i\pi)^3(-1)^i/6$
S-C	0	$(i\pi)(-1)^i/2$	0	$-i\pi(-1)^i/2$

Table 2
The coefficients of static beam functions under point-loads

Boundary condition	A_{0k}	A_{1k}	A_{2k}	A_{3k}
S-S	0	$(1-\xi_k)\xi_k(2-\xi_k)$	0	$-(1-\xi_k)$
C-C	0	0	$3\xi_k(1-\xi_k)^2$	$-(1-\xi_k)^2(1+2\xi_k)$
C-F	0	0	$3\xi_k$	-1
C-S	0	0	$-3(1-\xi_k)\xi_k(\xi_k-2)/2$	$(1-\xi_k)(\xi_k^2-2\xi_k-2)/2$
F-C	$(1-\xi_k)^2(2+\xi_k)$	$-3(1-\xi_k)^2$	0	0
S-C	0	$3(1-\xi_k)^2\xi_k/2$	0	$-(1-\xi_k)^2(2+\xi_k)/2$

where B_{ji} ($j = 0, 1, 2, 3$) are those for the C-F beam. Finally for an F-F beam, the static beam functions should be selected as

$$\phi_1(\xi) = 1,$$

$$\phi_2(\xi) = \xi \quad \text{or } \phi_2(\xi) = 1-\xi,$$

$$\phi_{i+2}(\xi) = B_{0i} + B_{1i}\xi + B_{2i}\xi^2 + B_{3i}\xi^3 + \sin i\pi\xi, \quad i \geqslant 1 \tag{1e}$$

where B_{ji} ($j = 0, 1, 2, 3$) are those for a C-F beam (or an F-C beam).

2.2. The static beam functions under a series of point-loads

Consider a beam acted upon by P static point-loads, the complete solution (Zhou, 1994) may be written as

$$z(\xi) = \sum_{k=1}^{P} P_k f_k(\xi), \tag{2a}$$

$$f_k(\xi) = A_{0k} + A_{1k}\xi + A_{2k}\xi^2 + A_{3k}\xi^3 + \left(\xi - \xi_{kj}\right)^3 U(\xi - \xi_k) \tag{2b}$$

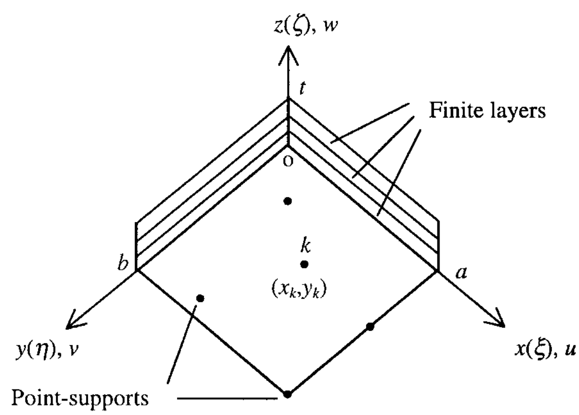

Fig. 1. A thick rectangular plate with point supports.

where $U(\xi - \xi_k)$ is the step function, P_k denotes the magnitude of the kth point-load and A_{ik} ($i = 0, 1, 2, 3$) are the unknown constants which can be determined by the boundary conditions of the beam (for a beam without rigid body motions) as shown in Table 2.

3. Finite layer formulation

A rectangular thick laminated composite plate with point supports is shown in Fig. 1. The plate is divided into a number of finite layers through the thickness. Each individual rectangular layer has two (L02) or three (H03) nodal surfaces. A suitable set of displacement functions is selected as

$$u(x, y, z) = \sum_{i=1}^{I} \sum_{j=1}^{J} \partial W_{ij}(x, y)/\partial x\big[N(z)\big]\{\alpha\}_{ij} \tag{3a}$$

$$\upsilon(x, y, z) = \sum_{i=1}^{I} \sum_{j=1}^{J} \partial W_{ij}(x, y)/\partial y\big[N(z)\big]\{\beta\}_{ij} \tag{3b}$$

$$w(x, y, z) = \sum_{i=1}^{I} \sum_{j=1}^{J} W_{ij}(x, y)\big[N(z)\big]\{\delta\}_{ij} \tag{3c}$$

where $W_{ij}(x, y)$ are the basic functions formed by the two sets of static beam functions, $[N(z)]$ denotes the one-dimensional linear (L02) or quadratic (H03) shape functions, I and J are truncated order of the displacement functions. The in-plane displacements along the x- and y-axes are defined by $\upsilon(x, y, z)$ and $\upsilon(x, y, z)$, respectively. The displacement unknowns are denoted by $\{\alpha\}_{ij}$, $\{\beta\}_{ij}$ and $\{\delta\}_{ij}$.

Using the above three equations, the strain–displacement relationships are derived as

$$\{\varepsilon\} = \begin{Bmatrix} \varepsilon_x \\ \varepsilon_y \\ \varepsilon_z \\ \gamma_{yz} \\ \gamma_{xz} \\ \gamma_{xy} \end{Bmatrix} = \sum_{i=1}^{I} \sum_{j=1}^{J} \begin{bmatrix} \dfrac{\partial^2 W_{ij}}{\partial x^2}[N] & 0 & 0 \\ 0 & \dfrac{\partial^2 W_{ij}}{\partial y^2}[N] & 0 \\ 0 & 0 & W_{ij}\left[\dfrac{\mathrm{d}N}{\mathrm{d}z}\right] \\ 0 & \dfrac{\partial W_{ij}}{\partial y}\left[\dfrac{\mathrm{d}N}{\mathrm{d}z}\right] & \dfrac{\partial W_{ij}}{\partial y}[N] \\ \dfrac{\partial W_{ij}}{\partial x}\left[\dfrac{\mathrm{d}N}{\mathrm{d}z}\right] & 0 & \dfrac{\partial W_{ij}}{\partial x}[N] \\ \dfrac{\partial^2 W_{ij}}{\partial x\,\partial y}[N] & \dfrac{\partial^2 W_{ij}}{\partial x\,\partial y}[N] & 0 \end{bmatrix} \begin{Bmatrix} \{\alpha\} \\ \{\beta\} \\ \{\gamma\} \end{Bmatrix}_{i,j}. \tag{4}$$

The stress–strain relationships are

$$\{\sigma\} = \{\sigma_x \quad \sigma_y \quad \sigma_z \quad \tau_{yz} \quad \tau_{xz} \quad \tau_{xy}\}^{\mathrm{T}} = [D]\{\varepsilon\} \tag{5}$$

where $[D]$ is the property matrix for materials as given in Appendix A. Applying the well-known

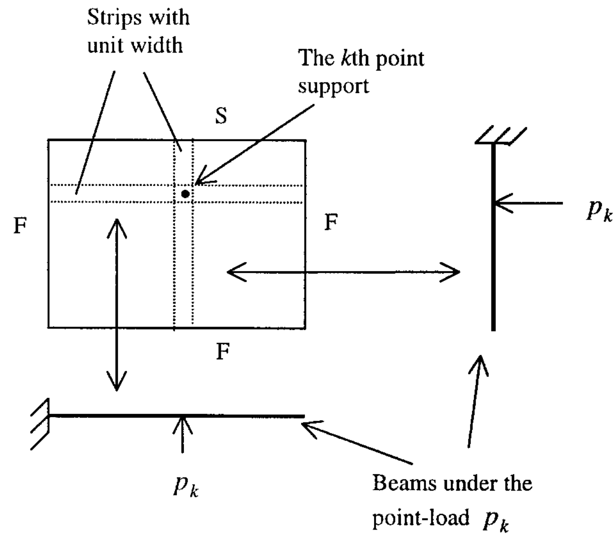

Fig. 2. The relations between point-loaded beams and the point-supported plate.

displacement method, the global stiffness and mass matrices can be easily formed by assembling the layer stiffness and mass matrices, as given in Appendix B, for each individual finite layer. Finally, eigenfrequencies and corresponding mode shapes can be extracted using standard procedures of eigenvalue analysis.

4. Basic functions

The basic functions $W_{ij}(x, y)$ which describe the variation of three-dimensional displacements of each finite layer in the x–y coordinate plate, must satisfy the prescribed geometrical boundary conditions of the plate, including the zero-displacement conditions at point supports. It is obvious that the conventional admissible functions such as the vibrating beam functions cannot be directly applied to this problem because of the existence of point supports. On the other hand, using the continuous beam vibrating functions as proposed by Cheung and Delcourt (1977) required rather lengthy computation and is therefore, inconvenient. Here the basic functions selected comprise of two parts, namely, the first part being the product of the one-dimensional static beam functions ($\phi_i(\xi)$, $\psi_j(\eta)$) under sinusoidal loads, while the second part is the product of the one-dimensional static beam function ($f_k(\xi)$, $g_k(\eta)$) under the kth point load. The basic functions can be written as

$$W_{ij}(\xi, \eta) = \phi_i(\xi)\psi_j(\eta) + \sum_{k=1}^{P} R_{ijk} f_k(\xi) g_k(\eta) \qquad (6)$$

where $\xi = z/a, \eta = y/b$ and P is the number of the point supports. $\phi_i(\xi)$ is the static beam function under the ith sinusoidal load component, as given by eqns (1b–e), which satisfies the corresponding boundary conditions of the plate in the ξ-direction but disregarding the point supports. $f_k(\xi)$ is the beam function under the kth point-load, as given by eqn (2b), which satisfies the corresponding boundary conditions of the plate in the ξ-direction and treating all point supports as point-loads. It should be noted that for beams with rigid body motions as shown in Fig. 2, boundary conditions of the type C-F or F-C should be used. The same principle applies to functions $\psi_j(\eta)$ and $g_k(\eta)$ in the η-direction. The unknown coefficients $R_{ijk}(k = 1, 2, \ldots, P)$ in eqn (6) are determined by the zero-displacement conditions of the plate at the P point-supports, as demonstrated below:

$$\Phi_{ij}(\xi_l, \eta_l) = \phi_i(\xi_l)\psi_j(\eta_l) + \sum_{k=1}^{P} R_{ijk} f_k(\xi_l) g_k(\eta_l) = 0, \tag{7a}$$

where (ξ_l, η_l) is the coordinate of the lth point-support of the plate. Consequently, the following linear simultaneous equations can be obtained

$$\begin{bmatrix} f_1(\xi_1)g_1(\eta_1) & f_2(\xi_1)g_2(\eta_1) & \cdots & f_P(\xi_1)g_P(\eta_1) \\ f_1(\xi_2)g_1(\eta_2) & f_2(\xi_2)g_2(\eta_2) & \cdots & f_P(\xi_2)g_P(\eta_2) \\ \vdots & \vdots & \vdots & \vdots \\ f_1(\xi_P)g_1(\eta_P) & f_2(\xi_P)g_2(\eta_P) & \cdots & f_P(\xi_P)g_P(\eta_P) \end{bmatrix} \begin{bmatrix} R_{ij1} \\ R_{ij2} \\ \vdots \\ R_{ijP} \end{bmatrix} = \begin{bmatrix} -\phi_i(\xi_1)\psi_j(\eta_1) \\ -\phi_i(\xi_2)\psi_j(\eta_2) \\ \vdots \\ -\phi_i(\xi_P)\psi_j(\eta_P) \end{bmatrix}, \tag{7b}$$

for every pair of i, j.

The solution of the above equation may be easily obtained as follows

$$\begin{bmatrix} R_{ij1} \\ R_{ij2} \\ \vdots \\ R_{ijP} \end{bmatrix} = \begin{bmatrix} f_1(\xi_1)g_1(\eta_1) & f_2(\xi_1)g_2(\eta_1) & \cdots & f_P(\xi_1)g_P(\eta_1) \\ f_1(\xi_2)g_1(\eta_2) & f_2(\xi_2)g_2(\eta_2) & \cdots & f_P(\xi_2)g_P(\eta_2) \\ \vdots & \vdots & \vdots & \vdots \\ f_1(\xi_P)g_1(\eta_P) & f_2(\xi_P)g_2(\eta_P) & \cdots & f_P(\xi_P)g_P(\eta_P) \end{bmatrix}^{-1} \begin{bmatrix} -\phi_i(\xi_1)\psi_j(\eta_1) \\ -\phi_i(\xi_2)\psi_j(\eta_2) \\ \vdots \\ -\phi_i(\xi_P)\psi_j(\eta_P) \end{bmatrix}. \tag{8}$$

On closer examination of eqns (3c) and (6), one can easily observe that the out-of-plane displacement $w(x, y, z)$ vanishes at the point supports across the thickness. This implies that a point support is equivalent to imposing rigid-line constraint to the vertical displacement $w(x, y, z)$ across the thickness. Obviously, for a plate without point supports (Zhou, 1996), all $R_{ijk}(k = 1, 2, \ldots, P)$ are equal to zero. Furthermore, because the coefficient matrix of $R_{ijk}(k = 1, 2, \ldots, P)$ is independent of the summing variables i and j, only one inverse calculation to the coefficient matrix in eqn (10) is required when solving the coefficients $R_{ijk}(k = 1, 2, \ldots, P)$ for all i and j. As a result, the computational cost is greatly reduced.

5. Numerical studies

The finite layer method developed in previous sections is applied to compute the non-dimensional frequency parameters, $\lambda = \omega(b/2)^2(\rho t/\sqrt{D_{11}D_{22}})^{1/2}$, for thick, laminated rectangular plates and $\lambda = \omega b^2\sqrt{\rho t/D}$ for isotropic thin plates, where ω is the circular frequency $D_{11} = E_1 t^3/[12(1 - \nu_{12}\nu_{21})]$ and $D_{22} = E_2 t^3/[12(1 - \nu_{12}\nu_{21})]$. It is obvious that $D_{11} = D_{22} = D = Et^3/[12(1 - \nu^2)]$ for isotropic plates. For laminated plates, the properties of material (Noor, 1973) are taken as follows: $E_1/E_2 = 40; G_{12}/E_2 = 0.6; G_{23}/E_2 = 0.5; G_{13} = G_{23}; \nu_{12} = \nu_{13} = 0.25$. The fibre orientations of different laminae alternate between 0 and 90° with respect to the x-axis. The influences of the plate aspect ratios ($\lambda = a/b$), side-to-thickness ratios (t/b), stacking sequences for laminated plates are examined. These results are, to the best of the author's knowledge, presented for the first time in open literature. It is noteworthy that for simply-supported plates with a central point-support, the vibration modes can be classified into four distinct categories, namely, double symmetric (SS) modes, symmetric–antisymmetric modes (SA), antisymmetric–symmetric modes (AS) and double antisymmetric modes (AA). Each of these categories is separately determined and thus, results in a smaller set of eigenfrequency equations. However, since the eigenfrequencies of the SA, AS and AA modes in this case are just the same as those of plates without the point support (Cheung and Chakrabarti, 1972; Liew et al., 1993), only the SS modes are computed. In the following examples, all finite layers are taken to be the same thickness and 24 Gaussian integration points are used for the integral computations in the x–y plane. For isotropic plates, $v = 0.3$ is assumed.

5.1. Convergence and comparison

The finite layer approach gives an upper-bound solution to the exact value. A convergence study is first carried out so as to ensure that the solutions to the problem are convergent and to establish the required number of terms in the three-dimensional displacement functions for obtaining satisfactory accuracy. In Table 3, convergence patterns of the first eight eigenfrequencies of the symmetric–symmetric mode for an isotropic homogeneous, simply-supported square plate with a central point-support are presented. It can be seen that the eigenfrequencies converge monotonically from above as the number of terms of basic functions and the number of L02 layers increase. A careful scrutiny of the convergence table reveals that the terms of the basic functions in the x–y plane play a more dominant role in the convergence and accuracy than the number of the layers in the z-direction both for thin and thick plates. The convergence rate for the thin plate ($t/b = 0.01$) is slightly faster than that for the thick plate ($t/b = 0.02$). In general, the comparison of the present results with those (Kim and Dickinson, 1987) obtained by the thin plate theory for the thin plate ($t/b = 0.01$) are better than those (Liew et al., 1994) obtained by the Mindlin plate theory for the thicker plate ($t/b = 0.02$). However, the difference is rather small and the maximum error is less than 2.1% for all cases. Moreover, from the table it is shown that using higher-order interpolation functions in the thickness direction of the layer can further improve the computational accuracy.

In Table 4, a comparative study of the first five eigenfrequencies of thin square plates ($t/b = 0.01$) with a corner-support (where symmetry does not exist) and with four corner-supports (where symmetry exists but not utilized in the computations) are given. The terms of displacement functions in the x- and y-directions and the number of L02 layers in the z-direction are taken as $5 \times 5 \times 5$. Comparison of the present results with those obtained by the thin plate theory (Mizusawa and Kajita, 1987; Kim and Dickinson, 1987) shows that good agreement is observed for all cases.

5.2. Numerical examples

From the convergence studies, it is found that the 7×7 terms of the displacement functions in the x–y plane and five L02 finite layers in the z-direction are sufficient to obtain satisfactory results for both thin plates and thick plates and they are used throughout the following computations.

The non-dimensional eigenfrequencies of symmetric–symmetric modes for the simply-supported isotropic rectangular plate with a central point-support are given in Table 5. The influences of aspect ratio and side-to-thickness ratio on the eigenfrequencies are studied. It is observed that for a plate with a prescribed aspect ratio, the non-dimensional eigenfrequencies, λ, decrease as the side-to-thickness ratio, t/b, increases, especially for the higher modes. Conversely, for a plate with a prescribed thickness ratio, the non-dimensional eigenfrequencies decrease as the aspect ratio, a/b, increases.

The second set of results is for a skew-symmetric rectangular laminate with a central point-support. It consists of two plies with 0/90° stacking sequences. In this case, symmetry of vibrating modes of the

Table 3
Convergence study of non-dimensional eigenfrequencies, $\lambda = \omega(b/2)^2\sqrt{\rho t/D}$ for isotropic homogeneous square thick plates with simply-supported edges and a central point-support

Thickness ratio t/b	Terms in x, y, z	Mode number							
		SS-1	SS-2	SS-3	SS-4	SS-5	SS-6	SS-7	SS-8
0.01	4 × 4 × 4	13.77	24.80	37.83	53.41	64.32	75.85	83.99	106.2
	4 × 4 × 5	13.74	24.74	37.74	53.29	64.15	75.66	83.78	106.0
	5 × 5 × 4	13.65	24.80	37.60	53.80	64.32	75.50	83.99	104.9
	5 × 5 × 5	13.62	24.74	37.52	52.96	64.15	75.32	83.78	104.6
	6 × 6 × 4	13.56	24.80	37.45	52.87	64.32	75.29	83.99	104.1
	6 × 6 × 5	13.53	24.74	37.36	52.75	64.15	75.11	83.78	103.9
	6 × 6 × 6	13.52	24.71	37.32	52.68	64.06	75.01	83.66	103.7
	7 × 7 × 5	13.38	24.74	37.25	52.60	64.15	74.96	83.78	103.3
	Kim and Dickinson (1987)	13.29	24.67	37.05					
0.1	4 × 4 × 4	11.88	21.58	29.97	36.46	40.23	45.35	48.05	53.81
	4 × 4 × 5	11.85	21.50	29.85	36.46	40.07	45.35	47.86	53.57
	5 × 5 × 4	11.69	21.58	29.62	36.11	39.88	45.23	48.05	53.45
	5 × 5 × 5	11.65	21.50	29.50	36.11	39.72	45.23	47.86	53.21
	6 × 6 × 4	11.54	21.58	29.36	35.88	39.63	45.15	48.05	53.19
	6 × 6 × 5	11.50	21.50	29.24	35.88	39.47	45.15	47.86	52.96
	6 × 6 × 6	11.48	21.46	29.17	35.88	39.38	45.15	47.74	52.83
	7 × 7 × 5	11.39	21.50	29.03	35.71	39.28	45.10	47.86	52.76
	7 × 7 × 3[a]	11.31	21.37	28.82	35.71	38.99	45.10	47.50	52.35
	Liew et al. (1994)	11.40	21.26	29.42					
0.2	4 × 4 × 4	9.125	16.72	18.23	21.24	22.62	27.60	32.54	32.81
	4 × 4 × 5	9.115	16.65	18.23	21.13	22.62	27.45	32.35	32.80
	5 × 5 × 4	8.962	16.72	18.05	20.96	22.56	27.38	32.54	32.62
	5 × 5 × 5	8.919	16.65	18.05	20.85	22.56	27.24	32.35	32.62
	6 × 6 × 4	8.817	16.72	17.94	20.74	22.52	27.24	32.49	32.54
	6 × 6 × 5	8.775	16.64	17.94	20.64	22.52	27.09	32.35	32.49
	6 × 6 × 6	8.751	16.60	17.94	20.58	22.52	27.00	32.24	32.49
	7 × 7 × 5	8.663	16.64	17.85	20.47	22.49	26.98	32.35	32.40
	7 × 7 × 3[a]	8.590	16.51	17.85	20.29	22.49	26.72	32.01	32.40
	Liew et al. (1994)	8.512	16.29		20.60				

[a] The quadratic interpolation in the z-direction is used for each layer.

plate still exists. The thickness of the two laminates is not identical. The thickness of the 0 and the 90° ply is taken as 3/5 and 2/5 of the total thickness of the plate, respectively. The first eight non-dimensional eigenfrequencies for the symmetric–symmetric modes are given in Table 6.

The final set of results is for a symmetric–symmetric rectangular laminate with a central point-support. It consists of three plies with 0/90/0° stacking sequences. It is obvious that symmetry also exists for such a plate. The thickness of each of the two outer 0° plies is taken as 2/5 of the total thickness, while the thickness of the middle 90° ply is taken as 1/5 of the total thickness. The firseight non-dimensional eigenfrequencies for the symmetric–symmetric modes are listed in Table 7 with different aspect ratio and side-to-thickness ratio.

It should be pointed out that the accuracy of the finite layer analysis can be improved by using quadratic (H03) instead of the linear (L02) interpolations. In Table 8 a comparative study is given for

Table 4
The first five non-dimensional eigenfrequencies, $\lambda = \omega b^2\sqrt{\rho t/D}$, of isotropic square thin plates with point supports at corners and different boundary conditions at the edges

Bound. con.	Methods	λ_1	λ_2	λ_3	λ_4	λ_5
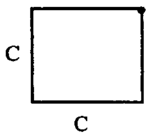	Present	15.59	24.51	40.32	55.52	64.98
	Mizusawa (1987)	15.12	23.70	39.37	53.53	62.54
	Kim (1987)	15.17	23.92	39.39	54.16	62.85
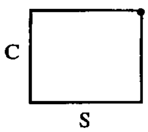	Present	12.17	21.73	35.64	48.42	60.28
	Mizusawa (1987)	11.94	21.06	35.01	47.24	57.92
	Kim (1987)	11.94	21.18	35.02	47.40	58.14
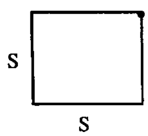	Present	9.724	17.54	30.83	44.41	52.71
	Mizusawa (1987)	9.608	17.32	30.60	43.65	51.04
	Kim (1987)	9.6079	17.316	30.596	43.652	51.051
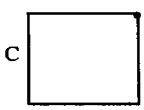	Present	5.427	16.31	22.45	29.95	44.50
	Mizusawa (1987)	5.312	15.86	21.71	29.29	43.39
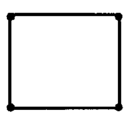	Present	7.246	15.85	15.85	20.07	39.92
	Mizusawa (1987)	7.111	15.77	15.77	19.60	38.43

Table 5
The first eight non-dimensional eigenfrequencies of symmetric–symmetric mode, $\lambda = \omega (b/2)^2\sqrt{\rho t/D}$, for isotropic thick plates with simply-supported edges and a central point-support

Aspect ratio a/b	Thickness ratio t/b	Mode number							
		SS-1	SS-2	SS-3	SS-4	SS-5	SS-6	SS-7	SS-8
1.0	0.10	11.38	21.50	29.03	35.71	39.28	45.10	47.86	52.76
	0.15	9.913	18.95	23.81	24.19	30.03	32.23	38.97	42.17
	0.20	8.663	16.64	17.85	20.47	22.49	26.98	32.35	32.40
	0.25	7.648	14.29	14.69	17.65	17.95	23.05	25.92	26.02
	0.30	6.825	11.90	13.08	14.91	15.46	20.05	21.57	21.60
1.5	0.10	7.520	15.26	22.37	26.24	29.79	32.76	38.31	40.54
	0.15	6.857	13.43	19.50	19.86	22.69	25.53	27.13	30.92
	0.20	6.208	11.83	14.89	17.00	19.13	19.64	22.86	23.18
	0.25	5.625	10.50	11.91	14.94	15.28	17.15	18.52	19.64
	0.30	5.117	9.404	9.927	12.12	13.26	15.15	15.41	17.15
2.0	0.10	5.453	11.61	17.80	21.83	25.66	26.72	29.39	34.97
	0.15	5.132	10.36	15.82	17.81	19.09	22.14	23.48	24.97
	0.20	4.781	9.210	13.36	14.00	16.68	17.60	18.71	19.14
	0.25	4.437	8.229	10.68	12.44	14.08	14.68	14.94	16.71
	0.30	4.115	7.409	8.903	11.13	11.73	12.43	13.04	14.76

Table 6
The first eight non-dimensional eigenfrequencies of symmetric-symmetric mode, $\lambda = \omega(b/2)^2(\rho t/\sqrt{D_{11}D_{22}})^{1/2}$, for skew-symmetric rectangular laminates with simply-supported edges and a central point-support

Aspect ratio a/b	Thickness ratio t/b	Mode number							
		SS-1	SS-2	SS-3	SS-4	SS-5	SS-6	SS-7	SS-8
1.0	0.10	7.286	14.60	18.00	22.95	28.27	30.44	32.67	35.86
	0.15	5.777	11.35	13.55	17.20	20.52	22.11	23.99	24.03
	0.20	4.789	9.215	10.83	13.72	16.00	16.43	17.39	18.95
	0.25	4.090	7.746	9.019	11.39	11.70	13.55	14.08	14.33
	0.30	3.568	6.679	7.723	9.075	9.771	10.80	11.52	12.15
1.5	0.10	5.193	10.01	15.67	16.80	19.75	23.66	26.37	29.48
	0.15	4.345	7.973	11.88	12.93	14.86	17.82	19.59	20.09
	0.20	3.695	6.604	9.502	10.48	11.87	13.99	14.25	15.54
	0.25	3.200	5.627	7.916	8.799	9.869	10.46	11.85	12.85
	0.30	2.816	4.897	6.786	7.580	8.158	8.503	9.979	10.14
2.0	0.10	4.059	7.647	11.95	15.68	16.72	18.26	20.88	23.83
	0.15	3.541	6.218	9.493	11.75	12.79	13.98	15.72	17.48
	0.20	3.085	5.211	7.823	9.374	10.30	11.29	12.47	12.66
	0.25	2.709	4.475	6.6398	7.802	8.607	9.442	9.580	10.47
	0.30	2.405	3.916	5.758	6.687	7.377	7.628	8.132	8.955

Table 7
The first eight non-dimensional eigenfrequencies of symmetric–symmetric mode, $\lambda = \omega(b/2)^2(\rho t/\sqrt{D_{11}D_{22}})^{1/2}$, for symmetric rectangular laminates with simply-supported edges and a central point-support

Aspect ratio a/b	Thickness ratio t/b	Mode number							
		SS-1	SS-2	SS-3	SS-4	SS-5	SS-6	SS-7	SS-8
1.0	0.10	7.328	13.19	20.88	22.12	25.73	30.94	35.19	35.59
	0.15	5.920	10.37	15.10	16.94	19.13	23.00	23.13	25.29
	0.20	4.896	8.580	11.76	13.66	15.39	16.76	18.27	19.40
	0.25	4.157	7.328	9.637	11.40	12.88	12.92	15.08	15.25
	0.30	3.609	6.398	8.161	9.768	10.27	11.14	11.33	12.72
1.5	0.10	5.657	9.216	13.95	19.76	20.73	22.45	25.22	27.14
	0.15	4.681	7.425	11.11	14.59	15.42	16.62	17.92	18.69
	0.20	3.937	6.164	9.244	11.29	12.31	13.26	13.38	14.86
	0.25	3.379	5.265	7.914	9.219	10.18	10.43	11.38	12.36
	0.30	2.954	4.599	6.914	7.792	8.528	8.678	9.847	10.57
2.0	0.10	5.105	7.102	10.50	14.45	18.93	20.50	21.27	22.88
	0.15	4.195	5.910	8.493	11.55	14.42	14.85	15.42	15.44
	0.20	3.513	4.988	7.086	9.622	11.13	11.50	11.75	12.48
	0.25	3.010	4.293	6.080	8.238	9.055	9.121	9.666	10.48
	0.30	2.630	3.761	5.328	7.190	7.524	7.639	8.216	9.739

Table 8
The convergence and comparison study of finite layer method for three-dimensional eigenvalues $\lambda = (\omega a^2)/\pi^2(\rho t/D)^2$ of an isotropic thick square plate with SSSS boundary conditions, $t/a = 0.5$, $\nu = 0.3$

Method	Terms in x, y, z	SS-1	SS-2	SS-3
Quadratic interpolation	$2 \times 2 \times 2$[a]	1.2630	1.8451	2.9351
	$2 \times 2 \times 3$	1.2598	1.8451	2.9330
	$2 \times 2 \times 4$	1.2592	1.8451	2.9326
	$2 \times 2 \times 5$	1.2591	1.8451	2.9325
Linear interpolation	$2 \times 2 \times 5$	1.2709	1.8451	2.9439
	$2 \times 2 \times 8$	1.2638	1.8451	2.9371
	$2 \times 2 \times 10$	1.2621	1.8451	2.9355
	$2 \times 2 \times 15$	1.2604	1.8451	2.9338
Rayleigh–Ritz[b]	$4 \times 4 \times 9$	1.2590	1.8451	2.9335

[a] The sequence of the terms is number of terms in x- and y-direction; number of finite layers in z-direction.
[b] From Liew, K.M., Hung, K.C., Lim, M.K., 1993. A continuum three-dimensional vibration analysis of thick rectangular plates. Int. J. Solids Struct. 30 (24), 3357–3379.

an isotropic thick plate with SSSS support conditions for linear interpolation (L02) and quadratic interpolation (H03). It can be seen that the results of the $2 \times 2 \times 3$ H03 analysis are already nearly exact and are better than those of the $2 \times 2 \times 15$ L02 analysis. It should be noted that be condensing the degrees-of-freedom associated with the H03 middle nodal surface there is very little difference in the amount of computational efforts between the L02 and H03 analysis.

6. Concluding remarks

A new set of two-dimensional basic functions has been developed by superimposing a set of static beam functions under sinusoidal loads to another set of beam functions under point loads. Unlike existing basic functions for vibration analysis of plates, this set of basic functions satisfies not only the geometric boundary conditions at the edges of the plate but also the zero out-of-plane deflection at the point supports. This new set of functions is combined with the finite layer method for the free vibration analysis of isotropic and laminated composite rectangular plates with point supports. Numerical results are compared with the thin-plate results for plates with different arrangement of point supports and good agreement is observed in all cases. To demonstrate the influence of aspect ratio, side-to-thickness ratio, material properties and stacking sequences on the vibrational behaviour of the plates with point supports, a simply-supported plate with a central point support is taken as an example to study idetail. Results for isotropic thick plates and laminated composite thick plates with two and three plies are summarized. To the best of the authors' knowledge, the information provided herein for three-dimensional vibration of thick plates with point supports is presented for the first time.

Appendix A

The property matrix $[D]$ for the composite materials with the fiber orientation angle θ with respect to the x-axis is

$$[D] = \begin{bmatrix} D_{11} & D_{12} & D_{13} & 0 & 0 & D_{16} \\ D_{12} & D_{22} & D_{23} & 0 & 0 & D_{26} \\ D_{13} & D_{23} & D_{33} & 0 & 0 & D_{36} \\ 0 & 0 & 0 & D_{44} & D_{45} & 0 \\ 0 & 0 & 0 & D_{45} & D_{55} & 0 \\ D_{16} & D_{26} & D_{36} & 0 & 0 & D_{66} \end{bmatrix}$$

where

$$D_{11} = Q_{11}m^4 + 2(Q_{12} + 2Q_{66})m^2n^2 + Q_{22}n^4,$$

$$D_{12} = (Q_{11} + Q_{22} - 4Q_{66})m^2n^2 + Q_{12}\left(m^4 + n^4\right),$$

$$D_{13} = Q_{13}m^2 + Q_{23}n^2,$$

$$D_{16} = -mn^3Q_{22} + m^3nQ_{11} - mn(m^2 - n^2)(Q_{12} + 2Q_{66}),$$

$$D_{22} = Q_{11}n^4 + 2(Q_{12} + 2Q_{66})m^2n^2 + Q_{22}m^4,$$

$$D_{23} = Q_{13}n^2 + Q_{23}m^2, \quad D_{33} = Q_{33},$$

$$D_{26} = -m^3nQ_{22} + mn^3Q_{11} + mn(m^2 - n^2)(Q_{12} + 2Q_{66}),$$

$$D_{36} = (Q_{13} - Q_{23})mn, \quad D_{44} = Q_{44}m^2 + Q_{55}n^2,$$

$$D_{45} = (Q_{55} - Q_{44})mn, \quad D_{55} = Q_{55}m^2 + Q_{44}n^2,$$

$$D_{66} = (Q_{11} + Q_{22} - 2Q_{12})m^2n^2 + Q_{66}(m^2 - n^2)^2$$

in which,

$$m = \cos(\theta), \; n = \sin(\theta)$$

and

$$Q_{11} = E_{11}(1 - v_{23}v_{32})/\Delta, \quad Q_{22} = E_{22}(1 - v_{31}v_{13})/\Delta,$$

$$Q_{33} = E_{33}(1 - v_{12}v_{21})/\Delta, \quad Q_{44} = G_{23}, \quad Q_{55} = G_{13},$$

$$Q_{66} = G_{12}, \quad Q_{12} = (v_{12} + v_{32}v_{13})E_{22}/\Delta,$$

$$Q_{13} = (v_{13} + v_{12}v_{23})E_{22}/\Delta, \quad Q_{23} = (v_{23} + v_{21}v_{13})E_{33}/\Delta,$$

$$\Delta = 1 - v_{12}v_{21} - v_{23}v_{32} - v_{31}v_{13} - 2v_{21}v_{32}v_{13}.$$

In the above equations, E_{11} and E_{22} are the Young's moduli parallel and perpendicular to the fibers, respectively and E_{33} is the Young's modulus in the thickness direction of the plate, G_{23}, G_{13} and G_{12} are the shear moduli of elasticity, v_{12}, v_{21}, v_{13}, v_{31}, v_{32} and v_{23} are the Poisson's ratios.

Appendix B

The layer stiffness matrix $[K]$ and mass matrix $[M]$ are written in the form of, respectively,

$$[K]=\begin{bmatrix}[K]_{1,1,1,1} & \dots & [K]_{1,1,1,J} & [K]_{1,1,2,1} & \dots & [K]_{1,1,I,J}\\ \vdots & \vdots & \vdots & \vdots & \vdots & \vdots\\ [K]_{1,J,1,1} & \dots & [K]_{1,J,1,J} & [K]_{1,J,2,1} & \dots & [K]_{1,J,I,J}\\ [K]_{2,1,1,1} & \dots & [K]_{2,1,1,J} & [K]_{2,1,2,1} & \dots & [K]_{2,1,I,J}\\ \vdots & \vdots & \vdots & \vdots & \vdots & \vdots\\ [K]_{I,J,1,1} & \dots & [K]_{I,J,1,J} & [K]_{I,J,2,1} & \dots & [K]_{I,J,I,J}\end{bmatrix}$$

$$[M]=\begin{bmatrix}[M]_{1,1,1,1} & \dots & [M]_{1,1,1,J} & [M]_{1,1,2,1} & \dots & [M]_{1,1,I,J}\\ \vdots & \vdots & \vdots & \vdots & \vdots & \vdots\\ [M]_{1,J,1,1} & \dots & [M]_{1,J,1,J} & [M]_{1,J,2,1} & \dots & [M]_{1,J,I,J}\\ [M]_{2,1,1,1} & \dots & [M]_{2,1,1,J} & [M]_{2,1,2,1} & \dots & [M]_{2,1,I,J}\\ \vdots & \vdots & \vdots & \vdots & \vdots & \vdots\\ [M]_{I,J,1,1} & \dots & [M]_{I,J,1,J} & [M]_{I,J,2,1} & \dots & [M]_{I,J,I,J}\end{bmatrix}$$

where

$$[K]_{ijkl}=\begin{bmatrix}[K_{11}] & [K_{12}] & [K_{13}]\\ [K_{21}] & [K_{22}] & [K_{23}]\\ [K_{31}] & [K_{32}] & [K_{33}]\end{bmatrix}_{ijkl},\quad i,k=1,2,\dots,I,\quad j,l=1,2,\dots,J,$$

$$[M]_{ijkl}=\begin{bmatrix}[M_{11}] & 0 & 0\\ 0 & [M_{22}] & 0\\ 0 & 0 & [M_{33}]\end{bmatrix}_{ijkl},\quad i,k=1,2,\dots,I,\quad j,l=1,2,\dots,J,$$

in which,

$$\begin{aligned}[K_{11}]_{ijkl}={}&D_{11}\int\!\!\int\frac{\partial^2 W_{ij}}{\partial x^2}\frac{\partial^2 W_{kl}}{\partial x^2}\,\mathrm{d}x\,\mathrm{d}y\int[N]^{\mathrm{T}}[N]\,\mathrm{d}z+D_{16}\int\!\!\int\frac{\partial^2 W_{ij}}{\partial x^2}\frac{\partial^2 W_{kl}}{\partial x\,\partial y}\,\mathrm{d}x\,\mathrm{d}y\int[N]^{\mathrm{T}}[N]\,\mathrm{d}z\\ &+D_{55}\int\!\!\int\frac{\partial W_{ij}}{\partial x}\frac{\partial W_{kl}}{\partial x}\,\mathrm{d}x\,\mathrm{d}y\int\left[\frac{\mathrm{d}N}{\mathrm{d}z}\right]^{\mathrm{T}}\left[\frac{\mathrm{d}N}{\mathrm{d}z}\right]\mathrm{d}z+D_{16}\int\!\!\int\frac{\partial^2 W_{ij}}{\partial x\,\partial y}\frac{\partial^2 W_{kl}}{\partial x^2}\,\mathrm{d}x\,\mathrm{d}y\int[N]^{\mathrm{T}}[N]\,\mathrm{d}z\\ &+D_{66}\int\!\!\int\frac{\partial^2 W_{ij}}{\partial x\,\partial y}\frac{\partial^2 W_{kl}}{\partial x\,\partial y}\,\mathrm{d}x\,\mathrm{d}y\int[N]^{\mathrm{T}}[N]\,\mathrm{d}z,\end{aligned}$$

$$[K_{12}]_{ijkl} = D_{12}\iint \frac{\partial^2 W_{ij}}{\partial x^2}\frac{\partial^2 W_{kl}}{\partial y^2}\,\mathrm{d}x\,\mathrm{d}y\int [N]^{\mathrm{T}}[N]\,\mathrm{d}z + D_{16}\iint \frac{\partial^2 W_{ij}}{\partial x^2}\frac{\partial^2 W_{kl}}{\partial x\,\partial y}\,\mathrm{d}x\,\mathrm{d}y\int [N]^{\mathrm{T}}[N]\,\mathrm{d}z$$
$$+ D_{45}\iint \frac{\partial W_{ij}}{\partial x}\frac{\partial W_{kl}}{\partial y}\,\mathrm{d}x\,\mathrm{d}y\int \left[\frac{\mathrm{d}N}{\mathrm{d}z}\right]^{\mathrm{T}}\left[\frac{\mathrm{d}N}{\mathrm{d}z}\right]\mathrm{d}z + D_{26}\iint \frac{\partial^2 W_{ij}}{\partial x\,\partial y}\frac{\partial^2 W_{kl}}{\partial y^2}\,\mathrm{d}x\,\mathrm{d}y\int [N]^{\mathrm{T}}[N]\,\mathrm{d}z$$
$$+ D_{66}\iint \frac{\partial^2 W_{ij}}{\partial x\,\partial y}\frac{\partial^2 W_{kl}}{\partial x\,\partial y}\,\mathrm{d}x\,\mathrm{d}y\int [N]^{\mathrm{T}}[N]\,\mathrm{d}z,$$

$$[K_{13}]_{ijkl} = D_{13}\iint \frac{\partial^2 W_{ij}}{\partial x^2}W_{kl}\,\mathrm{d}x\,\mathrm{d}y\int [N]^{\mathrm{T}}\left[\frac{\mathrm{d}N}{\mathrm{d}z}\right]\mathrm{d}z + D_{45}\iint \frac{\partial W_{ij}}{\partial x}\frac{\partial W_{kl}}{\partial y}\,\mathrm{d}x\,\mathrm{d}y\int \left[\frac{\mathrm{d}N}{\mathrm{d}z}\right]^{\mathrm{T}}[N]\,\mathrm{d}z$$
$$+ D_{55}\iint \frac{\partial W_{ij}}{\partial x}\frac{\partial W_{kl}}{\partial y}\,\mathrm{d}x\,\mathrm{d}y\int \left[\frac{\mathrm{d}N}{\mathrm{d}z}\right]^{\mathrm{T}}[N]\,\mathrm{d}z + D_{36}\iint \frac{\partial^2 W_{ij}}{\partial x\,\partial y}W_{kl}\,\mathrm{d}x\,\mathrm{d}y\int [N]^{\mathrm{T}}\left[\frac{\mathrm{d}N}{\mathrm{d}z}\right]\mathrm{d}z,$$

$$[K_{21}]_{ijkl} = D_{12}\iint \frac{\partial^2 W_{ij}}{\partial y^2}\frac{\partial^2 W_{kl}}{\partial x^2}\,\mathrm{d}x\,\mathrm{d}y\int [N]^{\mathrm{T}}[N]\,\mathrm{d}z + D_{26}\iint \frac{\partial^2 W_{ij}}{\partial y^2}\frac{\partial^2 W_{kl}}{\partial x\,\partial y}\,\mathrm{d}x\,\mathrm{d}y\int [N]^{\mathrm{T}}[N]\,\mathrm{d}z$$
$$+ D_{45}\iint \frac{\partial W_{ij}}{\partial y}\frac{\partial W_{kl}}{\partial x}\,\mathrm{d}x\,\mathrm{d}y\int \left[\frac{\mathrm{d}N}{\mathrm{d}z}\right]^{\mathrm{T}}\left[\frac{\mathrm{d}N}{\mathrm{d}z}\right]\mathrm{d}z + D_{16}\iint \frac{\partial^2 W_{ij}}{\partial x\,\partial y}\frac{\partial^2 W_{kl}}{\partial x^2}\,\mathrm{d}x\,\mathrm{d}y\int [N]^{\mathrm{T}}[N]\,\mathrm{d}z$$
$$+ D_{66}\iint \frac{\partial^2 W_{ij}}{\partial x\,\partial y}\frac{\partial^2 W_{kl}}{\partial x\,\partial y}\,\mathrm{d}x\,\mathrm{d}y\int [N]^{\mathrm{T}}[N]\,\mathrm{d}z,$$

$$[K_{22}]_{ijkl} = D_{22}\iint \frac{\partial^2 W_{ij}}{\partial y^2}\frac{\partial^2 W_{kl}}{\partial y^2}\,\mathrm{d}x\,\mathrm{d}y\int [N]^{\mathrm{T}}[N]\,\mathrm{d}z + D_{26}\iint \frac{\partial^2 W_{ij}}{\partial y^2}\frac{\partial^2 W_{kl}}{\partial x\,\partial y}\,\mathrm{d}x\,\mathrm{d}y\int [N]^{\mathrm{T}}[N]\,\mathrm{d}z$$
$$+ D_{44}\iint \frac{\partial W_{ij}}{\partial y}\frac{\partial W_{kl}}{\partial x}\,\mathrm{d}x\,\mathrm{d}y\int \left[\frac{\mathrm{d}N}{\mathrm{d}z}\right]^{\mathrm{T}}\left[\frac{\mathrm{d}N}{\mathrm{d}z}\right]\mathrm{d}z + D_{26}\iint \frac{\partial^2 W_{ij}}{\partial x\,\partial y}\frac{\partial^2 W_{kl}}{\partial y^2}\,\mathrm{d}x\,\mathrm{d}y\int [N]^{\mathrm{T}}[N]\,\mathrm{d}z$$
$$+ D_{66}\iint \frac{\partial^2 W_{ij}}{\partial x\,\partial y}\frac{\partial^2 W_{kl}}{\partial x\,\partial y}\,\mathrm{d}x\,\mathrm{d}y\int [N]^{\mathrm{T}}[N]\,\mathrm{d}z,$$

$$[K_{23}]_{ijkl} = D_{23}\iint \frac{\partial^2 W_{ij}}{\partial y^2}W_{kl}\,\mathrm{d}x\,\mathrm{d}y\int [N]^{\mathrm{T}}\left[\frac{\mathrm{d}N}{\mathrm{d}z}\right]\mathrm{d}z + D_{44}\iint \frac{\partial W_{ij}}{\partial y}\frac{\partial W_{kl}}{\partial y}\,\mathrm{d}x\,\mathrm{d}y\int \left[\frac{\mathrm{d}N}{\mathrm{d}z}\right]^{\mathrm{T}}[N]\,\mathrm{d}z$$
$$+ D_{45}\iint \frac{\partial W_{ij}}{\partial y}\frac{\partial W_{kl}}{\partial y}\,\mathrm{d}x\,\mathrm{d}y\int \left[\frac{\mathrm{d}N}{\mathrm{d}z}\right]^{\mathrm{T}}[N]\,\mathrm{d}z + D_{36}\iint \frac{\partial^2 W_{ij}}{\partial x\,\partial y}W_{kl}\,\mathrm{d}x\,\mathrm{d}y\int [N]^{\mathrm{T}}\left[\frac{\mathrm{d}N}{\mathrm{d}z}\right]\mathrm{d}z,$$

$$[K_{31}]_{ijkl} = D_{13}\iint W_{ij}\frac{\partial^2 W_{kl}}{\partial x^2}\,\mathrm{d}x\,\mathrm{d}y\int \left[\frac{\mathrm{d}N}{\mathrm{d}z}\right]^{\mathrm{T}}[N]\,\mathrm{d}z + D_{36}\iint W_{ij}\frac{\partial^2 W_{kl}}{\partial x\,\partial y}\,\mathrm{d}x\,\mathrm{d}y\int \left[\frac{\mathrm{d}N}{\mathrm{d}z}\right]^{\mathrm{T}}[N]\,\mathrm{d}z$$
$$+ D_{45}\iint \frac{\partial W_{ij}}{\partial y}\frac{\partial W_{kl}}{\partial x}\,\mathrm{d}x\,\mathrm{d}y\int [N]^{\mathrm{T}}\left[\frac{\mathrm{d}N}{\mathrm{d}z}\right]\mathrm{d}z + D_{55}\iint \frac{\partial W_{ij}}{\partial x}\frac{\partial W_{kl}}{\partial x}\,\mathrm{d}x\,\mathrm{d}y\int [N]^{\mathrm{T}}\left[\frac{\mathrm{d}N}{\mathrm{d}z}\right]\mathrm{d}z,$$

$$[K_{32}]_{ijkl} = D_{23}\iint W_{ij}\frac{\partial^2 W_{kl}}{\partial y^2}\,\mathrm{d}x\,\mathrm{d}y\int\left[\frac{\mathrm{d}N}{\mathrm{d}z}\right]^{\mathrm{T}}[N]\,\mathrm{d}z + D_{36}\iint W_{ij}\frac{\partial^2 W_{ij}}{\partial x\,\partial y}\,\mathrm{d}x\,\mathrm{d}y\int\left[\frac{\mathrm{d}N}{\mathrm{d}z}\right]^{\mathrm{T}}[N]\,\mathrm{d}z$$
$$+ D_{44}\iint \frac{\partial W_{ij}}{\partial y}\frac{\partial W_{kl}}{\partial y}\,\mathrm{d}x\,\mathrm{d}y\int[N]^{\mathrm{T}}\left[\frac{\mathrm{d}N}{\mathrm{d}z}\right]\mathrm{d}z + D_{45}\iint \frac{\partial W_{ij}}{\partial x}\frac{\partial W_{kl}}{\partial y}\,\mathrm{d}x\,\mathrm{d}y\int[N]^{\mathrm{T}}\left[\frac{\mathrm{d}N}{\mathrm{d}z}\right]\mathrm{d}z,$$

$$[K_{33}]_{ijkl} = D_{33}\iint W_{ij}W_{kl}\,\mathrm{d}x\,\mathrm{d}y\int\left[\frac{\mathrm{d}N}{\mathrm{d}z}\right]^{\mathrm{T}}\left[\frac{\mathrm{d}N}{\mathrm{d}z}\right]\mathrm{d}z + D_{44}\iint \frac{\partial W_{ij}}{\partial y}\frac{\partial W_{kl}}{\partial y}\,\mathrm{d}x\,\mathrm{d}y\int[N]^{\mathrm{T}}[N]\,\mathrm{d}z$$
$$+ D_{45}\iint \frac{\partial W_{ij}}{\partial y}\frac{\partial W_{kl}}{\partial x}\,\mathrm{d}x\,\mathrm{d}y\int[N]^{\mathrm{T}}[N]\,\mathrm{d}z + D_{45}\iint \frac{\partial W_{ij}}{\partial x}\frac{\partial W_{kl}}{\partial y}\,\mathrm{d}x\,\mathrm{d}y\int[N]^{\mathrm{T}}[N]\,\mathrm{d}z$$
$$+ D_{55}\iint \frac{\partial W_{ij}}{\partial x}\frac{\partial W_{kl}}{\partial x}\,\mathrm{d}x\,\mathrm{d}y\int[N]^{\mathrm{T}}[N]\,\mathrm{d}z,$$

$$[M_{11}]_{ijkl} = \rho\iint \frac{\partial W_{ij}}{\partial x}\frac{\partial W_{kl}}{\partial x}\,\mathrm{d}x\,\mathrm{d}y\int[N]^{\mathrm{T}}[N]\,\mathrm{d}z,$$

$$[M_{22}]_{ijkl} = \rho\iint \frac{\partial W_{ij}}{\partial y}\frac{\partial W_{kl}}{\partial y}\,\mathrm{d}x\,\mathrm{d}y\int[N]^{\mathrm{T}}[N]\,\mathrm{d}z,$$

$$[M_{33}]_{ijkl} = \rho\iint W_{ij}W_{kl}\,\mathrm{d}x\,\mathrm{d}y\int[N]^{\mathrm{T}}[N]\,\mathrm{d}z.$$

In the above equations, the double integrations are carried out over the entire surface of the plate and integration through the thickness of each layer is done separately, ρ is the density of the material.

References

Cheung, Y.K., Chakrabarti, S., 1972. Free vibration of thick, layered rectangular plates by finite layer method. Journal of Sound and Vibration 21, 277–284.

Cheung, Y.K., Delcourt, C., 1977. Buckling and vibration of thin, flat-walled structures continuous over several spans. Paper No. 7959, Part 2, Proc. Institution of Civil Engineers, pp. 39–103.

Cheung, Y.K., Tham, L.G., 1997. Finite Strip Method. CRC Press, LLC.

Dave, D.J., 1978. Finite strip models for vibration of Mindlin plates. Journal of Sound and Vibration 59, 441–452.

Fan, S.C., Cheung, Y.K., 1984. Flexural free vibrations of rectangular plates with complex support conditions. Journal of Sound and Vibration 93, 81–94.

Fan, J.R., Sheng, H.Y., 1992. The exact solution of laminated thick rectangular plates with clamped edges. Acta Mechanica Sinica 24, 574–582.

Fan, J.R., Ye, J.Q., 1990. An exact solution for the statics and dynamics of laminated thick plates with orthotropic layers. International Journal of Solids and Structures 26, 655–662.

Gorman, D.J., Singal, R.K., 1991. Analytical and experimental study of vibrating rectangular plates on rigid point supports. AIAA 29, 838–844.

Hanna, N.F., Leissa, A.W., 1994. A higher order shear deformation theory for the vibration of thick plates. Journal of Sound and Vibration 170, 545–555.

Kim, C.S., Dickinson, S.M., 1987. Flexural vibration of rectangular plates with point supports. Journal of Sound and Vibration 117, 249–261.

Leissa, A.W., 1969. Vibration of Plates, Washington, D.C.: Office of Technology Utilization, NASA. NASA SP-160.

Leissa, A.W., Zhang, Z.D., 1983. On the three-dimensional vibrations of the cantilevered rectangular parallelepiped. International Journal of Solids and Structures 73, 2013–2021.

Liew, K.M., Hung, K.C., Lim, M.K., 1993. A continuum three-dimensional vibration analysis of thick rectangular plates. International Journal of Solids and Structures 30, 3357–3379.

Liew, K.M., Hung, K.C., Lim, M.K., 1994. Three-dimensional plates: variance of simple support conditions and influence of in-plane inertia. International Journal of Solids and Structures 31, 3233–3247.

Liew, K.M., Xiang, Y., Kitipornchai, S., 1993. Transverse vibration of thick rectangular plates—I comprehensive sets of boundary conditions. Computers and Structures 49, 31–58.

Liew, K.M., Xiang, Y., Kitipornchai, S., Lim, M.K., 1994. Vibration of Mindlin plates on point supports using constraint functions. ASCE Journal of Engineering Mechanics 120, 499–513.

Mindlin, R.D., 1951. Influence of rotatory inertia and shear in flexural motion of isotropic, elastic plates. ASME Journal of Applied Mechanics 18, 1031–1036.

Mizusawa, T., Kajita, T., 1987. Vibration of skew plates resting on point supports. Journal of Sound and Vibration 115, 243–251.

Noor, A.K., 1973. Free vibrations of multilayered composite plates. AIAA 11, 1038–1039.

Reddy, J.N., 1984. A simple higher-order theory for laminated composite plates. ASME Journal of Applied Mechanics 51, 745–752.

Srinivas, S., Joga Rao, C.V., Rao, A.K., 1970. An exact analysis for vibration of simple-supported homogeneous and laminated thick rectangular plates. Journal of Sound and Vibration 12, 187–199.

Zhou, D., 1987. The application of a type of new admissible functions to the vibration of rectangular plates. Computers and Structures 52, 199–204.

Zhou, D., 1996. Natural frequencies of rectangular plates using a set of static beam functions in Rayleigh–Ritz method. Journal of Sound and Vibration 189, 81–87.